

# Approximate restoration of translational and rotational symmetries within the Lipkin method

Y. Gao (高原),<sup>1</sup> J. Dobaczewski,<sup>1,2,3</sup> and P. Toivanen<sup>1</sup>

<sup>1</sup>*Department of Physics, P.O. Box 35 (YFL), FI-40014 University of Jyväskylä, Finland*

<sup>2</sup>*Department of Physics, University of York, Heslington, York YO10 5DD, United Kingdom*

<sup>3</sup>*Helsinki Institute of Physics, P.O. Box 64, FI-00014 Helsinki, Finland*

**Background:** Nuclear self-consistent mean-field approaches are rooted in the density functional theory and, through the spontaneous symmetry breaking mechanism, allow for including important correlations, while keeping the simplicity of the approach. Because real ground states should have all symmetries of the nuclear Hamiltonian, these methods require subsequent symmetry restoration.

**Purpose:** We implement and study Lipkin method of approximate variation after projection applied to the restoration of the translational or rotational symmetries.

**Methods:** We use Lipkin operators up to quadratic terms in momenta or angular momenta with self-consistently determined values of the Peierls-Yoccoz translational masses or moments of inertia, respectively. Calculations based on Skyrme energy-density functional are performed for heavy, deformed, and paired nuclei.

**Results:** In deformed nuclei, the Peierls-Yoccoz translational masses along three different principal-axes directions of the intrinsic system can be different, which illustrates different widths of the total-momentum distributions. Numerically, the differences are only of the order of a few per cent. For the rotational-symmetry restoration, the Lipkin method compares favorably with the exact angular-momentum projection, which requires much larger computational effort.

**Conclusions:** The Lipkin method of translational and rotational symmetry restoration is a practical low-cost method of determining the corresponding correlation energies. It allows for a simultaneous restoration of several symmetries and can be relatively easily implemented in the standard self-consistent mean-field calculations, including those required for the parameter adjustments.

PACS numbers: 21.60.Jz, 21.10.Dr, 21.60.Ev

## I. INTRODUCTION

The self-consistent mean-field method based on nuclear density functional theory is an approach suitable for large-scale nuclear structure calculations, see, e.g., Refs. [1–6]. An important advantage of the mean-field method is that a many-body problem is transformed into a one-body problem, and that the wave function of the system can be represented by its one-body density derived from the Kohn-Sham Slater determinant [7]. The spontaneous symmetry breaking (SSB) [8] mechanism then allows for including important correlations, while keeping the simplicity of the approach. The SSB mechanism introduces symmetry-broken one-body densities and mean-field states. For example, by allowing nuclei to deform, quadruple correlations are included at the expense of broken rotational symmetry. Similarly, using the Bogoliubov transformation [8, 9], pairing correlations are taken into account, whereas the particle number is no longer conserved.

Although the use of the SSB mechanism is a big success of the mean-field method, it requires subsequent symmetry restoration [8], because real ground states should have all symmetries of the nuclear Hamiltonian conserved. This is realized by developing suitable projection methods, that is, by superposing wave functions with different values of the so-called generator coordinates [10], and thus building wave function with required conserved symmetries [11]. The projection can be performed after the variational process of solving the mean-field equations,

which is called projection after variation [11–13]. Another way is to perform the variation within the subset of projected wave functions, which is called variation after projection (VAP) [12, 14, 15]. Since energies of the projected states are still functionals of the unprojected densities, the VAP method also belongs to the class of density functional theories. However, as compared to projection after variation, computational cost of VAP is prohibitive, especially when several broken symmetries have to be simultaneously restored.

In practice, because of the large computational cost of projection methods, several approximate methods have already been developed. Examples of these are the center-of-mass and rotational corrections evaluated after variation [16–18]. The Lipkin VAP method [19], which we employ in this work, is also an approximate VAP method. Its key idea is to flatten the Hamiltonian so that the symmetry-conserving states with different quantum numbers become degenerate. Then, as a superposition, the symmetry-broken mean-field ground state gives the same energy as the ground state with the required symmetry conserved. This method has recently been successfully applied to the translational-symmetry restoration within the Hartree-Fock (HF) case [20] and to the particle-number restoration within the Hartree-Fock-Bogoliubov (HFB) calculations [21].

In the present study, we extend the translational-symmetry Lipkin VAP method of Ref. [20] to the case of deformed paired nuclei and fully implement the same method for the rotational-symmetry restoration. The pa-

per is organized as follows. In Sec. II, we present a general description of the Lipkin VAP method and we give some details regarding our implementation of the translational and rotational symmetry restoration. Results of calculations and conclusions are presented in Secs. III and IV, respectively.

## II. THEORY

For an operator  $\hat{O}$  that commutes with Hamiltonian  $\hat{H}$ , the mean-field state  $|\Phi\rangle$  can be written as a superposition of orthonormal eigenstates of  $\hat{O}$ :

$$|\Phi\rangle = \sum_i a_i |O_i\rangle. \quad (1)$$

The average energy of state  $|O_i\rangle$ , or the projected energy, is

$$E_i = \langle O_i | \hat{H} | O_i \rangle. \quad (2)$$

Here, we fix our attention on symmetry operators  $\hat{O}$  that have discrete spectra; however, a generalization to those having continuous spectra poses no problem.

Using Eqs. (1) and (2), the average of  $\hat{H}$  in the wave function  $|\Phi\rangle$  can be expressed as

$$E = \frac{\langle \Phi | \hat{H} | \Phi \rangle}{\langle \Phi | \Phi \rangle} = \frac{\sum_i |a_i|^2 E_i}{\sum_i |a_i|^2}. \quad (3)$$

Without any loss of generality, we can assume that for  $i = 0$  the eigenvalue of  $\hat{O}$  equals zero,  $O_0 = 0$ , and that  $E_i$  reaches its minimum at  $i = 0$ . Then one can always define a non-negative function  $f$ , such that  $f(0) = 0$  and

$$E_i = E_0 + f(O_i). \quad (4)$$

Inserting Eq. (4) into Eq. (3), one obtains

$$E = E_0 + \frac{\sum_i |a_i|^2 f(O_i)}{\sum_i |a_i|^2} = E_0 + \frac{\langle \Phi | f(\hat{O}) | \Phi \rangle}{\langle \Phi | \Phi \rangle}, \quad (5)$$

which gives,

$$E_0 = \frac{\langle \Phi | \hat{H} - f(\hat{O}) | \Phi \rangle}{\langle \Phi | \Phi \rangle}. \quad (6)$$

This means that one can obtain the projected energy  $E_0$  of the ground state  $|i=0\rangle$  by applying variational principle to the flattened Routhian  $\hat{H} - f(\hat{O})$  [19]. In the following, we refer to  $f(\hat{O})$  as the Lipkin operator.

One way to determine the form of  $f(\hat{O})$  is to expand it, for example, as an  $N$ -rank Taylor series,

$$f(\hat{O}) = \sum_{n=1}^N k_n \hat{O}^n, \quad (7)$$

and perform a polynomial fitting. As proposed by Lipkin [19], the simplest way to do that is by considering kernels of operators  $\hat{O}^n$ . Let  $\hat{Q}$  be an operator that commutes with both  $\hat{H}$  and  $\hat{O}$ , and  $q$  be a real parameter. Typically,  $\hat{Q}$  can be a generator of the symmetry group related to operator  $\hat{O}$ . Inserting the completeness relation  $1 = \sum_k |O_k\rangle\langle O_k|$  into the relation

$$\langle \Phi | \hat{H} e^{iq\hat{Q}} | \Phi \rangle = \sum_{ij} a_i^* a_j \langle O_i | \hat{H} e^{iq\hat{Q}} | O_j \rangle, \quad (8)$$

and using the fact that  $\hat{H}$ ,  $\hat{O}$ , and  $\hat{Q}$  commute with each other, one gets

$$\begin{aligned} \frac{\langle \Phi | \hat{H} e^{iq\hat{Q}} | \Phi \rangle}{\langle \Phi | e^{iq\hat{Q}} | \Phi \rangle} &= \frac{\sum_i |a_i|^2 E_i \langle O_i | e^{iq\hat{Q}} | O_i \rangle}{\sum_j |a_j|^2 \langle O_j | e^{iq\hat{Q}} | O_j \rangle} \\ &= \frac{\sum_i |a_i|^2 [E_0 + f(O_i)] \langle O_i | e^{iq\hat{Q}} | O_i \rangle}{\sum_j |a_j|^2 \langle O_j | e^{iq\hat{Q}} | O_j \rangle} \\ &= E_0 + \frac{\langle \Phi | f(\hat{O}) e^{iq\hat{Q}} | \Phi \rangle}{\langle \Phi | e^{iq\hat{Q}} | \Phi \rangle} \\ &= E_0 + \sum_{n=1}^N k_n \frac{\langle \Phi | \hat{O}^n e^{iq\hat{Q}} | \Phi \rangle}{\langle \Phi | e^{iq\hat{Q}} | \Phi \rangle}. \end{aligned} \quad (9)$$

If  $\langle \Phi | \hat{O}^n e^{iq\hat{Q}} | \Phi \rangle / \langle \Phi | e^{iq\hat{Q}} | \Phi \rangle$  is not a constant function of  $q$ , then changing the value of  $q$  one can obtain different values of kernels of  $\hat{O}^n$ . Therefore, to determine values of all parameters  $k_n$ , that is, to perform the  $N$ -rank polynomial fitting, one simply needs to consider  $N + 1$  different values of  $q_m$ ,  $m = 0, \dots, N$ , with  $q_0 = 0$ , and solve the problem of  $N + 1$  linear equations,

$$\frac{\langle \Phi | \hat{H} e^{iq_m \hat{Q}} | \Phi \rangle}{\langle \Phi | e^{iq_m \hat{Q}} | \Phi \rangle} = \sum_{n=0}^N k_n \frac{\langle \Phi | \hat{O}^n e^{iq_m \hat{Q}} | \Phi \rangle}{\langle \Phi | e^{iq_m \hat{Q}} | \Phi \rangle}, \quad (10)$$

where  $k_0 \equiv E_0$ .

When Taylor expansion (7) is reduced to the first power only ( $N = 1$ ), the  $2 \times 2$  equation (10) can be easily solved [20], which gives,

$$k = \frac{\langle \Phi | \hat{H} e^{iq\hat{Q}} | \Phi \rangle \langle \Phi | \Phi \rangle - \langle \Phi | \hat{H} | \Phi \rangle \langle \Phi | e^{iq\hat{Q}} | \Phi \rangle}{\langle \Phi | \hat{O} e^{iq\hat{Q}} | \Phi \rangle \langle \Phi | \Phi \rangle - \langle \Phi | \hat{O} | \Phi \rangle \langle \Phi | e^{iq\hat{Q}} | \Phi \rangle}, \quad (11)$$

where  $k \equiv k_1$  and  $q \equiv q_1$ . However, even when a few terms are kept in the Taylor expansion [21], the solution poses no problem either. Similarly, when the Lipkin operator contains not one but several operators  $\hat{O}$ , the combined linear equations will still have quite low dimensions. In practical cases, equations pertaining to different operators may turn out to be fairly well decoupled, and can be solved independently. This is, in fact, the case in our practical applications to translational-symmetry restoration, where shifts in three Cartesian directions are well decoupled from one another, and can be treated separately.

When  $\hat{O}$  is chosen to be  $\hat{Q}^2$ , it is possible to use the Gaussian overlap approximation (GOA) [8] to obtain estimates of kernels  $\langle \Phi | \hat{Q}^{2n} e^{iq\hat{Q}} | \Phi \rangle / \langle \Phi | e^{iq\hat{Q}} | \Phi \rangle$ . Within the GOA, we have

$$\langle \Phi | e^{iq\hat{Q}} | \Phi \rangle \approx e^{-\frac{1}{2}aq^2}, \quad a \equiv \langle \Phi | \hat{Q}^2 | \Phi \rangle. \quad (12)$$

From this, one can find that

$$\begin{aligned} \frac{\langle \Phi | \hat{Q}^{2n} e^{iq\hat{Q}} | \Phi \rangle}{\langle \Phi | e^{iq\hat{Q}} | \Phi \rangle} &= (-)^n \frac{d^{2n}}{dq^{2n}} \langle \Phi | e^{iq\hat{Q}} | \Phi \rangle \\ &\approx (-)^n e^{\frac{1}{2}aq^2} \frac{d^{2n}}{dq^{2n}} e^{-\frac{1}{2}aq^2} = \left(-\frac{a}{2}\right)^n H_{2n} \left(\sqrt{\frac{a}{2}}q\right), \end{aligned} \quad (13)$$

where  $H_{2n}$  is the Hermite polynomial of order  $2n$ . In addition, from expression (12),  $a$  can be calculated from the following formula,

$$a \approx -2 \lim_{q \rightarrow 0} \frac{\ln(\langle \Phi | e^{iq\hat{Q}} | \Phi \rangle)}{q^2}. \quad (14)$$

In this work, for the translational-symmetry restoration,  $f(\hat{O})$ ,  $\hat{Q}$ , and  $q$  are chosen as:

$$f = \sum_{i=x,y,z} k_i \hat{P}_i^2, \quad \hat{Q} = \hat{P}_{i=x,y,z}, \quad q = \delta x, \delta y, \delta z, \quad (15)$$

where  $\hat{P}_i$  are components of the total momentum operator in three Cartesian directions. In this way, for  $i = x, y, z$ , operator  $e^{iq\hat{Q}}$  shifts the nucleus by the distance of  $\delta x, \delta y, \delta z$  in the direction of the  $x, y, z$  axis, respectively. Three different operators  $\hat{Q}$  are used to make sure that kernels of squares of the total momentum in each direction,  $\langle \Phi | \hat{P}_i^2 e^{iq\hat{Q}} | \Phi \rangle / \langle \Phi | e^{iq\hat{Q}} | \Phi \rangle$ , do really change with shifts  $q$ .

The form of the Lipkin operator  $f(\hat{O})$  adopted for the translational-symmetry restoration is motivated by the following arguments. First, we expect that the energy expectation value has a similar form as the energy of the center-of-mass motion, which is  $\hat{\mathbf{P}}^2/2M$  [19]. However, since we consider deformed nuclei, dispersion of the total momentum can be anisotropic, and thus the three Lipkin parameters  $k_i$  can be different. Second, terms linear in momentum should disappear, because we study ground states of even-even nuclei and thus the time-reversal symmetry is not broken. Third, higher order terms are expected to be very small [20], and anyhow their implementation would have been very complicated.

For the rotational-symmetry restoration, in this paper we concentrate on axially deformed even-even nuclei. Therefore,  $f(\hat{O})$ ,  $\hat{Q}$ , and  $q$  are now chosen as:

$$f = k \left( \hat{J}_x^2 + \hat{J}_y^2 \right), \quad \hat{Q} = \hat{J}_y, \quad q = \beta, \quad (16)$$

where the axial-symmetry axis is aligned with the Cartesian  $z$  direction,  $\hat{J}_x$  and  $\hat{J}_y$  are the  $x$  and  $y$  components of

the total angular momentum, respectively, and  $\beta$  is the Euler rotation angle about the  $y$ -axis.<sup>1</sup> Here, operator  $e^{iq\hat{Q}}$  rotates the nucleus by angle  $\beta$  around the  $y$  axis. As in the translational case, because of the conserved time-reversal symmetry, linear terms are dropped. However, the fact that we neglect here higher-order terms restricts the present application to the case of collective rotation with energy increasing as square of the total angular momentum. By the same token, since the energy of an axial nucleus does not increase with increasing rotation about the symmetry axis, in the Lipkin operator we dropped the term  $\hat{J}_z^2$ . Anyhow, in the ground state of an even-even axial nucleus, the average value of this term vanishes,  $\langle \hat{J}_z^2 \rangle = 0$ .

### III. RESULTS AND DISCUSSION

Implementations of the approximate restoration of translational and rotational symmetries within the Lipkin method were here carried out using the code HFODD (v2.73m) [22, 23], which solves the HFB equations on a 3D Cartesian harmonic oscillator basis. All calculations were performed in the space of 16 major spherical harmonic-oscillator shells and with the Skyrme SLy4 parametrization [24]. For the HFB calculations, a volume zero-range pairing interaction with a cutoff window of  $E_{\text{cut}} = 60$  MeV was used. For the translational case, we only performed calculations with pairing, and the pairing strengths were adjusted to reproduce experimental odd-even mass staggering in the entire rare-earth region, which gave  $V_n = -159$  MeV fm<sup>3</sup> for neutrons and  $V_p = -152$  MeV fm<sup>3</sup> for protons. For the rotational case, we performed calculations both with and without pairing correlations included. Here, the pairing strengths were adjusted to reproduce experimental odd-even mass staggering in nuclei around <sup>168</sup>Er, which gave  $V_n = -202.17$  and  $V_p = -221.70$  MeV fm<sup>3</sup>. To improve the convergence when solving the HFB equations, the two-basis method [22, 25] was used.

#### A. Restoration of the translational symmetry

As discussed in Ref. [20], coefficients  $k_i$  that define the Lipkin operator (15) correspond to the so-called Peierls-Yoccoz masses [11] and characterize the momentum contents of the symmetry-broken stationary ground-state wave function. Conversely, the exact inertial mass  $m_A$  characterizes the reaction of the system to the boost (an increase in momentum). As it turns out, both masses

<sup>1</sup> Depending on the context, the same symbol  $\beta$  is traditionally used both for the second Euler angle and Bohr deformation, which must not be confused.

have similar but not identical values [20]. In the present work we represent the calculated values of  $k_i$  through the ratios of the corresponding Peierls-Yoccoz and exact masses, that is,

$$R_i = \frac{M_{PY,i}}{mA} = \frac{1}{2k_i mA} \quad \text{for } i = x, y, z. \quad (17)$$

Needless to say that in deformed nuclei, the momentum contents in the three Cartesian directions of the intrinsic system can be different, and thus the three Peierls-Yoccoz masses  $M_{PY,i}$  can be different too.

The effectiveness of the chosen Lipkin operator  $f(\hat{O})$  (15), used in the translational-symmetry restoration, can be tested by checking an eventual dependence of the Lipkin parameters  $k_{x,y,z}$  on shifts  $\delta x, \delta y, \delta z$ . In Fig. 1 we show this dependence for  $^{168}\text{Er}$ . One can see that when the shifts change from 0.05 to 1.5 fm, the Lipkin mass does not change much. This indicates that the quadratic shape is already a good approximation of the total momentum contents of the HFB wave function. In the following calculations, we fix the shifts at 0.5 fm.

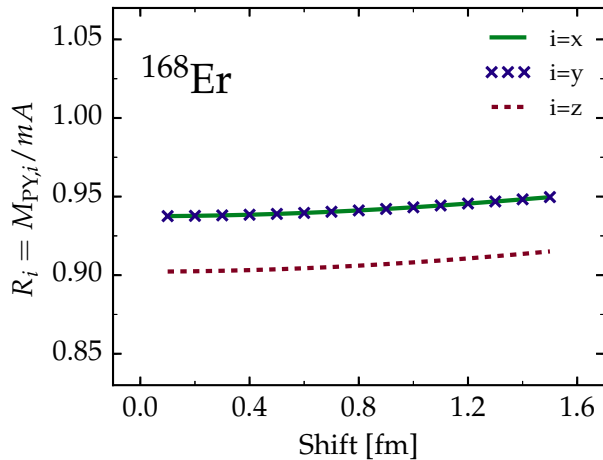


FIG. 1: Ratios (17) between the Peierls-Yoccoz masses in the  $x$ ,  $y$ , and  $z$  directions and the exact mass as functions of shifts in the corresponding directions, calculated for  $^{168}\text{Er}$ .

In Fig. 2(a), we plotted the average values of  $R_x$  and  $R_y$ ,

$$R_{(x+y)/2} \equiv \frac{1}{2}(R_x + R_y), \quad (18)$$

which characterize the overall values of the Peierls-Yoccoz masses in the directions perpendicular to the symmetry axis. As we can see, the Peierls-Yoccoz masses vary fairly smoothly with particle numbers and are almost unaffected by deformations of nuclei. Similarly, the Lipkin VAP energies (6), Fig. 2(b), smoothly overestimate the standard HFB energies, where the one-body center-of-mass corrections have been used [20, 26].

In Figs. 3(a) and 4(a), to illustrate the anisotropy of the Peierls-Yoccoz masses, we plotted differences of ratios (17),

$$R_{(x+y)/2-z} \equiv \frac{1}{2}(R_x + R_y) - R_z, \quad (19)$$

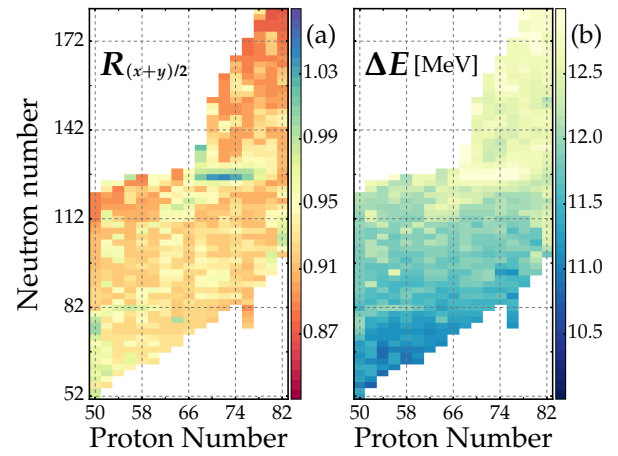


FIG. 2: (a) Average ratios of the Peierls-Yoccoz and exact masses in the  $x$  and  $y$  directions (18). (b) Differences  $\Delta E$  between the Lipkin VAP energies and those obtained within the standard HFB calculations.

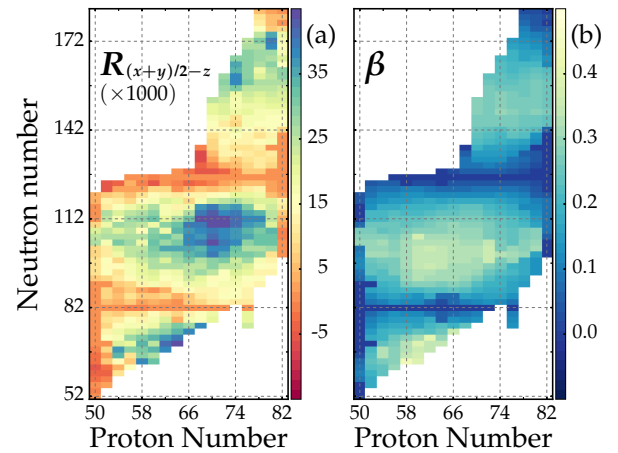


FIG. 3: (a)  $R_{(x+y)/2} - R_z$ : The difference between  $R_{(x+y)/2}$  and the mass ratio in the  $z$ -direction. (b) Beta deformations.

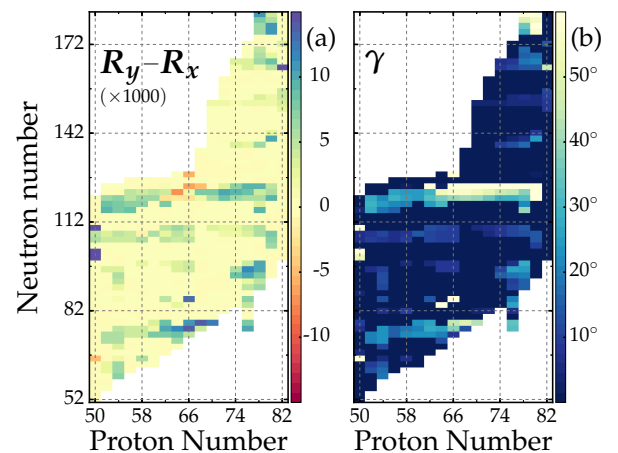


FIG. 4: (a)  $R_y - R_x$ : The difference between the mass ratios in the  $y$ - and  $x$ -directions. (b) Gamma deformations.

and  $R_y - R_x$ , respectively. First we note that the overall degree of the anisotropy is fairly small, with the above differences not exceeding a few per cent. Differences (19) characterize the anisotropy between the directions perpendicular and parallel to the symmetry axis, and very nicely correlate with values of deformations  $\beta$ , plotted in Fig. 3(b). Similarly, differences  $R_y - R_x$  correlate with the nonaxiality of shapes, as illustrated by values of deformations  $\gamma$ , plotted in Fig. 4(b).

### B. Restoration of the rotational symmetry

We begin by showing, in Fig. 5, spectra of well-deformed,  $^{168}\text{Er}$ , and weakly-deformed,  $^{190}\text{Er}$ , nucleus, calculated using the angular-momentum projection (AMP) of the standard HFB solutions. The results indicate a rotational mode of the former and a vibrational mode of the latter [8]. This means that in weakly-deformed nuclei, the parabolic Lipkin operator  $f(\hat{O})$  (16) may not be appropriate to flatten the total energy. Guided by these results, below we consider only well-deformed erbium isotopes with  $N = 86-118$ , with some weakly-deformed nuclei still included for possible further comparisons.

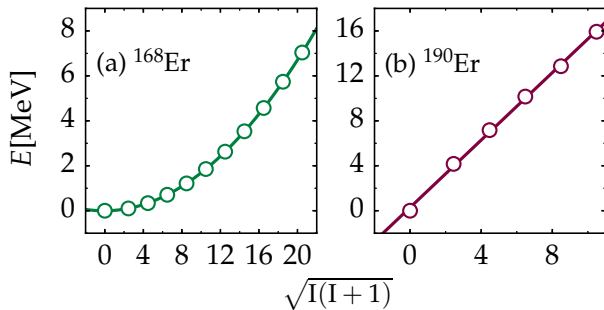


FIG. 5: Spectra of (a)  $^{168}\text{Er}$  and (b)  $^{190}\text{Er}$ . The angular momentum projection was performed after the convergence of the standard HFB calculation.

All results below are shown for the Lipkin parameters  $k$  re-represented in terms of the Lipkin Moments of Inertia (MoI)  $\mathcal{J}$  as

$$\mathcal{J} \equiv \frac{1}{2k}. \quad (20)$$

Similarly as in the case the translational symmetry, we begin by checking the dependence of results on the Euler rotation angle  $\beta$ . Since in well-deformed and weakly-deformed nuclei, the dependence of total energy on total angular momentum is different, in Fig. 6 we show the MoI determined in  $^{168}\text{Er}$  and  $^{190}\text{Er}$  as functions of the Euler rotation angle  $\beta$ . For both nuclei, we show results obtained with and without pairing correlations included. We found that in all cases, the Lipkin MoI very weakly depend on  $\beta$ . Therefore, results presented below were obtained using  $\beta = 0.1$ .

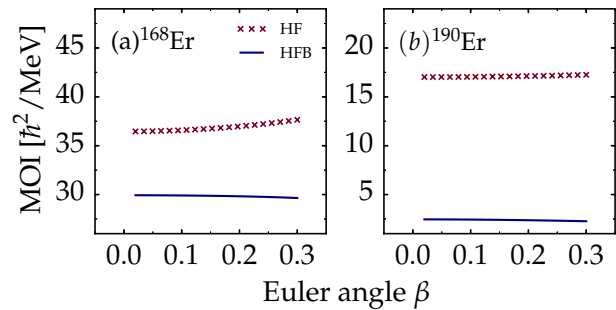


FIG. 6: The Lipkin MoI (20) determined for (a)  $^{168}\text{Er}$  and (b)  $^{190}\text{Er}$ , plotted as functions of the Euler rotation angle  $\beta$ .

In Fig. 7, we show energy corrections obtained by the Lipkin VAP, AMP after the convergence of the standard mean-field calculations, and AMP after the convergence of the Lipkin VAP calculations. In the case of calculations without pairing, Fig. 7(a), the results obtained by all three methods are quite similar. With pairing, Fig. 7(b), the same is true for results obtained by the Lipkin VAP and AMP after Lipkin VAP. A general agreement between the results of Lipkin VAP and AMP after Lipkin VAP supports the validity of the Lipkin VAP method as an approximation of the exact VAP method.

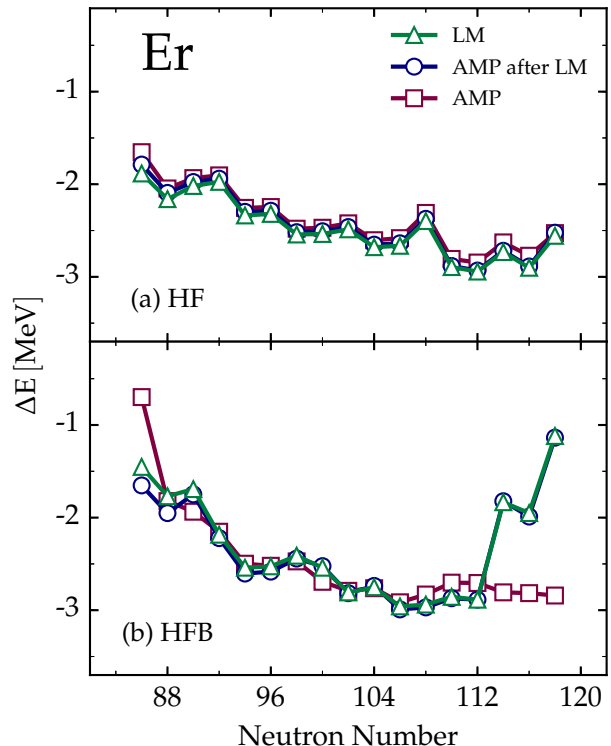


FIG. 7: Energy corrections obtained by the Lipkin VAP method (LM), AMP, and AMP after LM for erbium isotopes (a) without or (b) with pairing correlations.

In  $^{154,182-186}\text{Er}$ , owing to changes in deformation, marked differences appear between the standard and Lip-

kin VAP calculations with pairing. For example, as seen in the neutron Nilsson diagram for  $^{180}\text{Er}$ , Fig. 8, the intruder orbit  $\nu[660]_{1/2}^+$  crosses the extruder orbit  $\nu[503]_{7/2}^-$ . Thus in  $^{182-186}\text{Er}$ , the competition between the two configurations leads to different shapes obtained in the standard HFB and Lipkin methods. This is substantiated in Fig. 9, where we plotted occupation probabilities  $v^2$  of these two orbits in  $^{182-186}\text{Er}$ . By occupying the intruder orbit, the nuclei are driven to larger deformations.

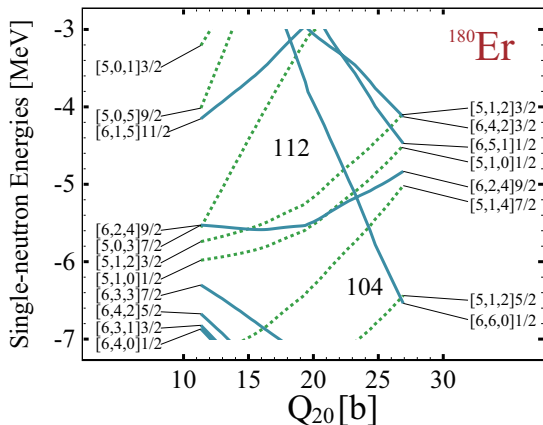


FIG. 8: Neutron Nilsson diagram for  $^{180}\text{Er}$ . Single-particle levels were determined as eigenenergies of the mean fields obtained using the deformation-constrained HFB calculations.

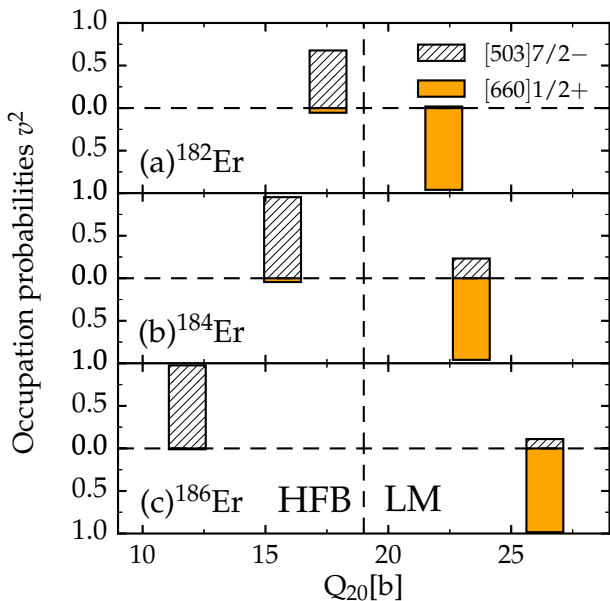


FIG. 9: Occupation probabilities  $v^2$  of neutron orbitals  $\nu[660]_{1/2}^+$  and  $\nu[503]_{7/2}^-$  in (a)  $^{182}\text{Er}$ , (b)  $^{184}\text{Er}$ , and (c)  $^{186}\text{Er}$ , determined within the HFB (left panel) and Lipkin (right panel) methods.

In Fig. 10, we compare the MoI calculated within the Lipkin VAP with those determined using the cranking method. The cranking calculations were performed at the frequency of  $\omega = 0.05\text{ MeV}$  and the first MoI were extracted as ratios of average angular momentum and frequency. Without pairing, the cranking MoI are significantly larger than those obtained using the Lipkin VAP. Once again, this is because they are two different quantities, corresponding to the Thouless-Valatin and Peierls-Yoccoz MoI, respectively [8]. The former illustrate how the system reacts to rotation, whereas the latter characterize average energies of components with good total angular momentum within a non-rotating broken-symmetry ground state. As it turns out, when the pairing is included, differences between the cranking and Lipkin VAP MoI become much smaller.

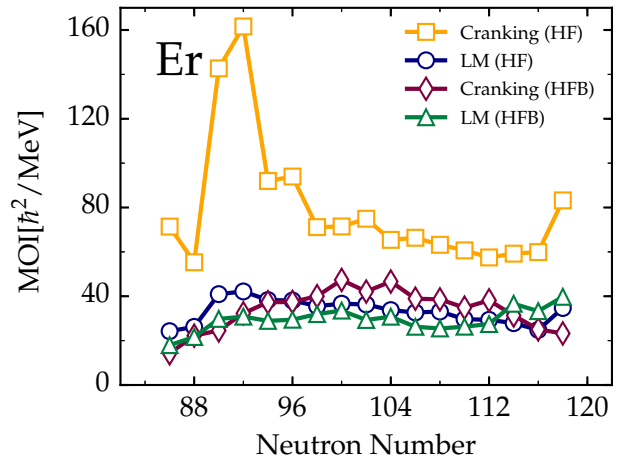


FIG. 10: MoI obtained using the Lipkin VAP method (LM) and cranking method with pairing correlations included (HFB) or not included (HF).

#### IV. CONCLUSIONS

In the present study, we applied the Lipkin method of the translational and rotational symmetry restoration so as to approximate the exact variation-after-projection method. We implemented the Lipkin method by constructing corrective Lipkin operators up to quadratic terms in linear and angular momenta, and we self-consistently determined the corresponding Peierls-Yoccoz translational masses and moments of inertia, respectively.

For the translational symmetry restoration, we performed calculations for even-even isotopes of elements with  $50 \leq Z \leq 82$ . We found that the Peierls-Yoccoz masses in different principal-axes directions of the intrinsic system differ up to a few per cent, which illustrates differences in linear-momentum distributions in deformed nuclei. For the rotational symmetry restoration, we performed calculations for even-even erbium isotopes. Here

we found that the correlation energies obtained within the Lipkin method nicely reproduce results of the exact angular-momentum projection.

### Acknowledgments

This work was supported in part by the Academy of Finland and University of Jyväskylä within the FIDIPRO

program, by the Polish National Science Center under Contract No. 2012/07/B/ST2/03907, and by the ERANET-NuPNET grant SARFEN of the Polish National Centre for Research and Development (NCBiR). We acknowledge the CSC-IT Center for Science Ltd., Finland, for the allocation of computational resources.

- 
- [1] M.V. Stoitsov, J. Dobaczewski, W. Nazarewicz, S. Pittel, and D.J. Dean, *Phys. Rev. C* **68**, 054312 (2003).
- [2] J.-P. Delaroche, M. Girod, J. Libert, H. Goutte, S. Hilaire, S. Péru, N. Pillet, and G.F. Bertsch, *Phys. Rev. C* **81**, 014303 (2010).
- [3] J. Erler, N. Birge, M. Kortelainen, W. Nazarewicz, E. Olsen, A. M. Perhac, and M. Stoitsov, *Nature* **486**, 509 (2012).
- [4] J. Erler, C.J. Horowitz, W. Nazarewicz, M. Rafalski, and P.-G. Reinhard, *Phys. Rev. C* **87**, 044320 (2013).
- [5] S.E. Agbemava, A.V. Afanasjev, D. Ray, and P. Ring, *Phys. Rev. C* **89**, 054320 (2014).
- [6] S. Goriely, *Nucl. Phys. A* **933**, 68 (2015).
- [7] W. Kohn and L.J. Sham, *Phys. Rev.* **140**, A1133 (1965).
- [8] P. Ring and P. Schuck, *The Nuclear Many-Body Problem* (Springer-Verlag, Berlin, 1980).
- [9] J.P. Blaizot and G. Ripka, *Quantum theory of finite systems*, MIT Press, Cambridge Mass., 1986.
- [10] H. Flocard and D. Vautherin, *Phys. Lett. B* **55**, 259 (1975).
- [11] R.E. Peierls and J. Yoccoz, *Proc. Phys. Soc. London*, **A70**, 381 (1957).
- [12] M. Bender, P.-H. Heenen, and P.-G. Reinhard, *Rev. Mod. Phys.* **75**, 121 (2003).
- [13] H. Zduńczuk, J. Dobaczewski, and W. Satuła, *Int. J. Mod. Phys. E* **16**, 377 (2007).
- [14] J.A. Sheikh, P. Ring, E. Lopes, and R. Rossignoli, *Phys. Rev. C* **66**, 044318 (2002).
- [15] M.V. Stoitsov, J. Dobaczewski, R. Kirchner, W. Nazarewicz, and J. Terasaki, *Phys. Rev. C* **76**, 014308 (2007).
- [16] F. Tondeur, S. Goriely, J.M. Pearson, and M. Onsi, *Phys. Rev. C* **62**, 024308 (2000).
- [17] J. Erler, P. Klüpfel, and P.-G. Reinhard, *J. Phys. G: Nucl. Part. Phys.* **38**, 033101 (2011).
- [18] Y. Nogami, *Phys. Rev.* **134** (1964) B313.
- [19] H.J. Lipkin, *Ann. of Phys.*, **9**, 272 (1960).
- [20] J. Dobaczewski, *J. Phys. G: Nucl. Part. Phys.* **36**, 105105 (2009).
- [21] X.B. Wang, J. Dobaczewski, M. Kortelainen, L.F. Yu, and M.V. Stoitsov, *Phys. Rev. C* **90**, 014312 (2014).
- [22] N. Schunck, J. Dobaczewski, J. McDonnell, W. Satuła, J.A. Sheikh, A. Staszczak, M. Stoitsov, and P. Toivanen, *Comput. Phys. Commun.* **183**, 166 (2012).
- [23] N. Schunck *et al.*, unpublished.
- [24] E. Chabanat, P. Bonche, P. Haensel, J. Meyer, and R. Schaeffer, *Nucl. Phys. A* **635**, 231 (1998); [Erratum, *ibid. A* **643**, 441 (1998)].
- [25] B. Gall, P. Bonche, J. Dobaczewski, H. Flocard, and P.-H. Heenen, *Z. Phys. A* **348**, 183 (1994).
- [26] M. Bender, K. Rutz, P.-G. Reinhard, and J.A. Maruhn, *Eur. Phys. Jour.* **A7**, 467 (2000).